ENVIRONMENTAL ENGINEERING SCIENCE
Volume 40, Number 11, 2023

DOI: 10.1089/ees.2023.0054

Interfacial Interactions of Uranium and Arsenic with Microplastics: From Field Detection to Controlled Laboratory Tests

Jasmine Quiambao,[1,†] Kendra Z. Hess,[2,†,‡] Sloane Johnston,[2] Eliane El Hayek,[3] Achraf Noureddine,[4] Abdul-Mehdi S. Ali,[5] Michael Spilde,[5] Adrian Brearley,[5] Peter Lichtner,[6] José M. Cerrato,[1,6,‡] Kerry J. Howe,[1,6,‡] and Jorge Gonzalez-Estrella[2,*,‡]

[1]*Department of Civil, Construction & Environmental Engineering, University of New Mexico, Albuquerque, New Mexico, USA.*
[2]*School of Civil & Environmental Engineering, Oklahoma State University, Stillwater, Oklahoma, USA.*
[3]*Department of Pharmaceutical Sciences, University of New Mexico, College of Pharmacy, Albuquerque, New Mexico, USA.*
[4]*Department of Chemical & Biological Engineering, University of New Mexico, Albuquerque, New Mexico, USA.*
[5]*Department of Earth and Planetary Sciences, University of New Mexico, Albuquerque, New Mexico, USA.*
[6]*Center for the Water and the Environment, University of New Mexico, Albuquerque, New Mexico, USA.*

Received: February 24, 2023 *Accepted in revised form: April 28, 2023*

Abstract

We studied the co-occurrence of microplastics (MPs) and metals in field sites and further investigated their interfacial interaction in controlled laboratory conditions. First, we detected MPs in freshwater co-occurring with metals in rural and urban areas in New Mexico. Automated particle counting and fluorescence microscopy indicated that particles in field samples ranged from 7 to 149 particles/L. The urban location contained the highest count of confirmed MPs, including polyester, cellophane, and rayon, as indicated by Attenuated Total Reflectance—Fourier Transform Infrared (ATR-FTIR) spectroscopy analyses. Metal analyses using inductively coupled plasma (ICP) revealed that bodies of water in a rural site affected by mining legacy contained up to 332.8 μg/L of U, while all bodies of water contained As concentrations below 11.4 μg/L. These field findings motivated experiments in laboratory conditions, reacting MPs with 0.02–0.2 mM of As or U solutions at acidic and neutral pH with poly(methyl-methacrylate), polyethylene, and polystyrene MPs. In these experiments, As did not interact with any of the MPs tested at pH 3 and pH 7, nor U with any MPs at pH 3. Experiments supplied with U and MPs at pH 7 indicated that MPs served as substrate surface for the adsorption and nucleation of U precipitates. Chemical speciation modeling and microscopy analyses (i.e., Transmission Electron Microscopy [TEM]) suggest that U precipitates resemble sodium-compreignacite and schoepite. These findings have relevant implications to further understanding the occurrence and interfacial interaction of MPs and metals in freshwater.

Keywords: arsenic; freshwater; microplastics; surface precipitation; uranium

Introduction

Microplastics (MPs), plastic materials <5 mm, are widely distributed in the marine environment; however, more information is needed to understand the prevalence of MPs in freshwater (Ateia et al., 2022; Blettler et al., 2018; Carbery et al., 2018). MPs in aquatic environments have been shown to cause a variety of toxic effects to marine biota, interact with other aquatic pollutants, and cause risk of human ingestion through trophic transfer (Godoy et al., 2019).

According to previous studies, MP concentrations in surface water range from 10^{-5} to 1,000 particles/L (Li et al., 2018). MP contamination in freshwater is closely related to anthropogenic activities and enters freshwater ecosystems through several sources, including littering, leaching, and runoff from landfills, or water treatment plants (Eerkes-Medrano et al., 2015). Higher concentrations of MPs prevail in areas with high population density or proximity to urban

**Corresponding author:* School of Civil & Environmental Engineering, Oklahoma State University, 248 Engineering North, Stillwater, OK 74078, USA. *E-mail:* jorgego@okstate.edu
†Both these authors contributed equally to the development of this article.
‡Member of AEESP.

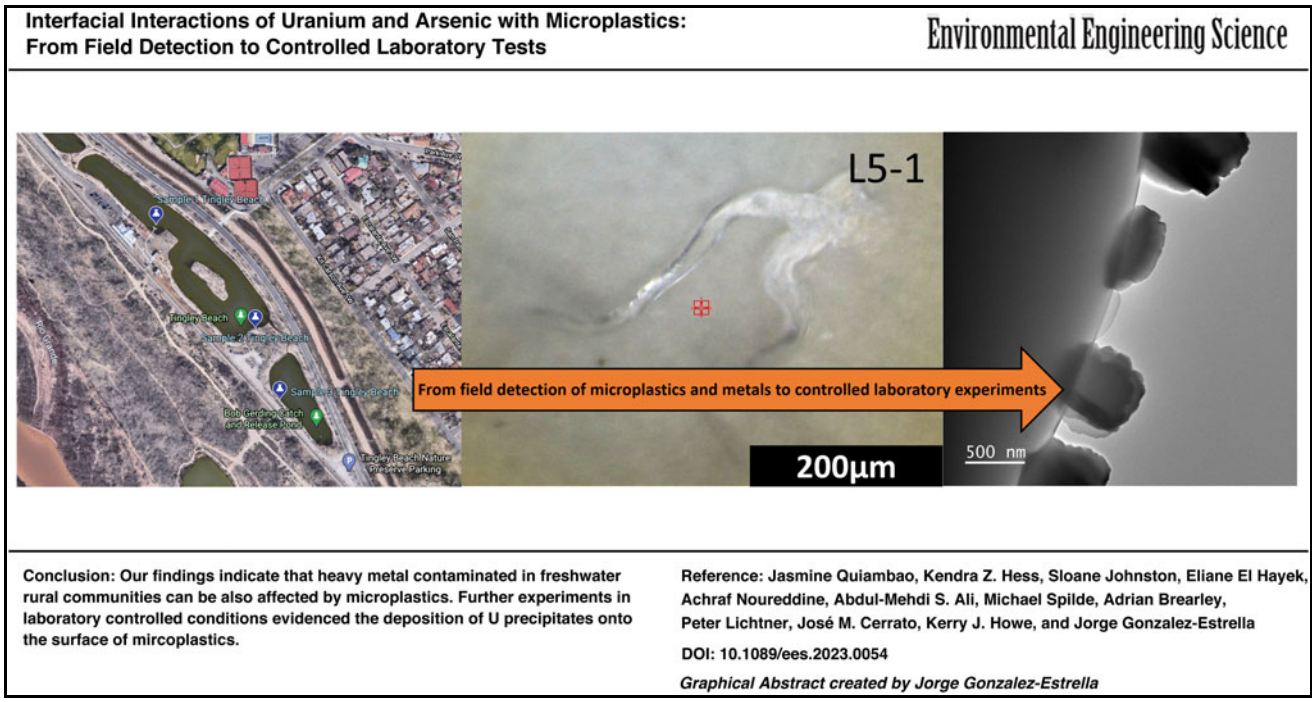

centers (Wong et al., 2020; Yonkos et al., 2014); nevertheless, MPs occur even in remote locations (Yang et al., 2021).

In freshwater, MPs interact with other contaminants (e.g., heavy metals); for example, aged polyvinyl chloride (PVC) MPs found in seawater showed traces of copper (Cu) and zinc (Zn) (Brennecke et al., 2016). Various metals were found sorbed in polyethylene terephthalate (PET), high-density polyethylene (HDPE), PVC, low-density polyethylene (LDPE), and polypropylene (PP) (Rochman et al., 2014); plastic materials such as PVC, HDPE, and LDPE adsorbed trace metals of Cu, Zn, Cd, and Pb in nine urban intertidal regions in Canada (Munier and Bendell, 2018). Heavy metals have been found on MPs; therefore, the potential of MPs reacting with heavy metals through sorption, complexation, or precipitation reactions increases in waters contaminated with heavy metals. However, we have limited information about the status of MP contamination in freshwater with known elevated concentrations of heavy metals.

The interaction between MPs and heavy metals is driven by physicochemical properties of MPs, chemical characteristics of heavy metals, and environmental conditions (Ateia et al., 2022; Tourinho et al., 2019). Organic matter, pH, ionic strength, salinity, contact time, and temperature affect the adsorption behavior of different contaminants on MPs as well (Nafiaah, 2020). Uranium and As undergo a wide range of complexation, dissociation, and precipitation reactions in water (Gonzalez-Estrella et al., 2020; Meza et al., 2023), and likely affect the typical sorption mechanisms between other metals and MPs observed in previous studies. Thus, more information is needed to understand the interfacial interactions of U and As with MPs.

Our study assessed the prevalence of MPs in urban and rural freshwater with known elevated U and As concentrations documented since 2014 and affected by U mining for a few decades (Blake et al., 2017; Blake et al., 2015). The field results motivated the evaluation of the interactions of As and U with polyethylene (PE), polystyrene (PS), and polymethyl (meta)acrylate (PMMA) MPs in controlled laboratory conditions. The novelty of our study is rooted in integrating field and laboratory methods to better understand the mechanisms affecting the interaction of metals and MPs. We provide new insights into the role of interfacial processes affecting the reactivity of metals and MPs in freshwater containing these constituents.

Materials and Methods

Field sampling and analyses

Quality control and quality assurance. The use of plastic materials was reduced as much as possible to avoid MP background contamination. All experimental instruments and glassware were sonicated for 30 min in an ultrasonic bath with ultra-pure water (18 MΩ) and covered with aluminum foil between sonication and use. All benchtops were carefully cleaned, and all laboratory procedures were conducted in a fume hood. Field controls were included to monitor any airborne contamination. In laboratory procedures, a control containing only ultra-high purity water during filtering and digestion was included to account for any background MP interference.

Sampling Methodology. For MP analyses, three 1-L samples were collected from six locations along Paguate River and freshwater reservoirs near the Jackpile Mine of Laguna Pueblo, NM. These sites were selected based on their proximity to the mine and the Laguna community. In addition, three locations on the Rio Grande, and three on Tingley Beach, Albuquerque, NM, were selected to compare occurrence of MPs in a rural and an urban community (Supplementary Table S1 in the Supplementary Data). Samples were taken from the first 10 cm of the water surface to avoid sediment interference. A separate set of samples was taken from

20 bodies of water in the area to confirm elevated concentrations of U and As reported in previous studies from our group (Blake et al., 2017; Blake et al., 2015). Note that less samples were taken for MP analyses due to the complexity of the extraction procedures.

Extraction of MPs. To extract MPs onto filters and ensure the quality of visual assessment and polymer identification, the procedure recommended by Koelmans et al. (2019) was followed. Details about the extraction of MP are provided in the Supplementary Data.

Analyses of MPs and metals in field samples. Filters containing extracted particles were examined and imaged using a stereomicroscope (AmScope 7X-180X Trinocular Zoom Stereo Microscope) for initial visual assessment. The filters were imaged using a fluorescence microscope (Cytation 5 Cell Imaging Multi Mode Reader; Agilent Technologies) with Gen5® software. For quantification, each filter's overall image was run through the MPVAT 2.0 macros using ImageJ (Prata et al., 2020). Each filter was then analyzed using an Attenuated Total Reflectance—Fourier Transform Infrared (ATR-FTIR) spectrometer (micro-FTIR, Thermo Nicolet iN10 MX). For each filter, the number of particles examined with ATR was 10% of the particles identified during fluorescence microscopy quantification, or a minimum of five (whichever was greater). Further details of the fluorescence and ATR-FTIR analyses are provided in the Supplementary Data.

Controlled laboratory experiments

Reagents. Sodium arsenate dibasic heptahydrate, $Na_2HAsO_47H_2O$ reagent (≥98%), was purchased from Sigma-Aldrich. Uranyl nitrate hexahydrate reagent, $UO_2(NO_3)_26(H_2O)$ (98–102%), was purchased from IBI Labs. Three types of MPs were used in these experiments: PE, PS, and PMMA (Supplementary Table S2 in the Supplementary Data). We selected the MP types based on their predominant abundance in the environment according to previous research (Di and Wang, 2018; Li et al., 2020).

We considered particles with different densities to have a representative distribution of plastics that potentially occur in the water column (Lenaker et al., 2019). PE (0.96 g/cc, 10–63 μm) and PMMA MPs (1.2 g/cc, 1–45 μm) were purchased from Cospheric. PS is used for packaging, disposable cups, and many other uses (Andrady and Neal, 2009). PS beads (200–300 μm) were purchased from Polysciences. Glass microfiber filters (Advantec GC-50 borosilicate diameter, 47 mm; Pore Size: 0.5 μm) were purchased from Cole-Parmer. The main characteristics of these MPs are provided in Supplementary Table S2 in the Supplementary Data.

Sorption experiments. These series of experiments were performed to assess the sorption of different concentrations of As and U onto PE, PS, and PMMA commercial MPs at pH 3 and pH 7. pH adjustments were made with 0.1 M HNO_3 or NaOH. A mass of 0.1 g of PE, PS, and PMMA commercial MPs was added into a borosilicate glass beaker containing a volume of 100 mL of deionized water, resulting in a concentration of 1 g MP/L, the concentration of MP to be within range (0.04–10 g/L) with other studies that evaluated the sorption of metals onto MP (Brennecke et al., 2016; Godoy et al., 2019; Holmes et al., 2014; Zou et al., 2020). Isotherms were carried out for 48 h by separately exposing the MPs to 0.05, 0.1, and 0.2 mM of U or As.

All experimental conditions were run in triplicates in a VWR Advanced Orbital Shaker Model 15000 at 150 rpm at room temperature (25°C) for 48 h. Controls without MPs and only including either U or As were included in the experiments.

The equilibrium time was selected based on kinetic experiments (Supplementary Fig. S3 in the Supplementary Data) and in our previous study where we observed rapid precipitation (<1 h) and equilibrium of soluble U after 48 h using a similar concentration range (0.005–1 mM of U) (Gonzalez-Estrella et al., 2020). On the other hand, the concentration for U and As was based on (1) being within the range of concentrations of U and As that we have found in Laguna Pueblo, NM, since 2013 (Blake et al., 2017; Blake et al., 2015) and other studies that have evaluated concentration of with U and As in U mine tailings (Donahue and Hendry, 2003; Robertson et al., 2019); and (2) ensuring we achieve saturation on the MP in case the sorption followed a typical adsorption behavior.

After 48 h, the solutions were vacuum filtered through a 0.5 μm glass microfiber filter and glass frit filter unit. The filtered water samples were transferred into centrifuge tubes and the filters were placed in a petri dish and stored at 4°C. Metal adsorption was determined by quantifying the soluble concentration of U and As with Inductively Coupled Plasma-Optical Emission Spectroscopy (ICP-OES) and ICP-Mass Spectroscopy (ICP-MS). Each filter paper was slowly rinsed with ultra-pure water (18 MΩ) to avoid additional compounds precipitating as the remaining water evaporated from the filter surface and preserved for spectroscopy analyses.

Interaction of MPs with filtered solutions of U. An additional set of experiments was conducted to isolate the interactions between soluble U and MPs at pH 7. In these experiments, 0.02 and 0.06 mM U were used and all U solutions were filtered before exposure to the MPs to eliminate U precipitates from the solution. PP centrifuge tubes were used instead of glass to ensure that the glass was not providing a surface for heterogenous precipitation. The isotherms were run with the same parameters and conditions explained above. Controls with no MP and only including either U or As were also included in the experiment.

Characterization of MPs. PE, PMMA, and PS MPs exposed to U and As were analyzed with various spectroscopy techniques to identify any precipitation reaction on the surface. Transmission Electron Microscopy (TEM), Scanning Electron Microscopy (SEM), and Energy Dispersive Spectroscopy (EDS) were used to examine the MP morphology and quantify heavy metals binding onto the surface. Zeta potential ζ was used to measure the surface charge of MPs at pH 3 and pH 7. Details of sample preparation and SEM and TEM analyses parameters are provided in the Supplementary Data.

Results and Discussion

Occurrence of MPs in freshwater

Quantification and characterization of MPs. All locations contained a similar range of particle concentrations (Table 1).

Table 1. Number of Particles Detected and Analyzed by ATR-FTIR, Including the Polymer Type and Their Percentage Matches in Laguna Pueblo, Tingley Beach, and the Rio Grande, New Mexico

Site	*Particles quantified*	*Particles analyzed*	*Particle tag*	*Polymer type*	*Match (%)*
Laguna Pueblo Fishing Pond (L1)	25	5	L1-1	Polyamide—Nylon 6/12	50
			L1-2	Urethane Alkyd, Linseed Oil-Rich	43
			L1-3	Precipitated Silica	42
			L1-4	Acrylonitrile Butadiene Styrene Terpolymer #6	39
			L1-5	Aromatic Hydrocarbon Resin	37
Laguna Pueblo, Rio Paguate (L2)	34	5	**L2-1**	**Cellophane**	**67**
			L2-2	Ponomer Resin #2	50
			L2-3	Poly(Styrene:Vinylidene Chloride)	37
			L2-4	Precipitated Silica	37
			L2-5	Di-(Methylthio) Toluene Diamine	29
Laguna Pueblo, Wetland (L3)	149	15	L3-1	Cellophane	44
			L3-2	Poly(Styrene:Vinylidene Chloride)	44
			L3-3	Cellophane	43
			L3-4	Cellophane	41
			L3-5	Cellophane	40
			L3-6	Cellophane	37
			L3-7	Cellophane	37
			L3-8	Cellophane	37
			L3-9	Cellophane	34
			L3-10	Polystyrene #4	33
			L3-11	Rayon	32
			L3-12	Poly(Styrene:4-Vinylpyridine)	32
			L3-13	Cellophane	30
			L3-14	2-(2-Hydroxy-3,5-(1,1 Dimethyl-benzylphenyl)Benzotriazole)	28
			L3-15	Zinc Borate Hydrate	25
Laguna Pueblo, Wetland Creek (L4)	82	8	L4-1	Rayon	50
			L4-2	Titanium Oxide (98%), Aluminum Oxide (2%)	44
			L4-3	Titanium Oxide (98%), Aluminum Oxide (2%)	44
			L4-4	Poly(Styrene:Vinyldiene Chloride)	42
			L4-5	Styrene Derived Plasticizer	42
			L4-6	Titanium Oxide (98%), Aluminum Oxide (2%)	39
			L4-7	Poly(Styrene:Vinylidene Chloride)	38
			L4-8	Propylene Glycol Dibenzoate #1	29
Laguna Pueblo. Creek near to Jackpile Mine (L5)	7	5	**L5-1**	**Rayon**	**72**
			L5-2	Poly(Styrene:Vinyldiene Chloride)	48
			L5-3	Acrylonitrile Butadiene Styrene Terpolymer #6	46
			L5-4	Cellophane	36
			L5-5	Cellophane	33
Laguna Pueblo. Creek near to Jackpile Mine (L6)	119	12	L6-1	Cellophane	50
			L6-2	Cellophane	50
			L6-3	Cellophane	50
			L6-4	Cellophane	48
			L6-5	Cellophane	48
			L6-6	Cellophane	47
			L6-7	Zinc Borate Hydrate	35
			L6-8	Barium Metaborate	33
			L6-9	Polyol Acetal	28
			L6-10	Barium Metaborate	27
			L6-11	Fluorocarbon	23
			L6-12	5-Phenyltetrazole, Calcium Salt	21
Tingley Beach, Albuquerque (T1)	18	5	**T1-1**	**Rayon**	**67**
			T1-2	**Cellophane**	**64**
			T1-3	**Cellophane**	**63**
			T2-4	Cellophane	51
			T2-5	Basic Lead Carbonate	35

(*continued*)

TABLE 1. (CONTINUED)

Site	*Particles quantified*	*Particles analyzed*	*Particle tag*	*Polymer type*	*Match (%)*
Tingley Beach, Albuquerque (T2)	43	5	**T2-1**	**Polyester**	**73**
			T2-2	**Polyester**	**73**
			T2-3	**Rayon**	**63**
			T2-4	Cellophane	53
			T2-5	2-Amino-2-Methyl-1-Propanol #1	47
Tingley Beach, Albuquerque (T3)	127	13	**T3-1**	**Polytetrafluoroethylene #4**	**65**
			T3-2	**Cellophane**	**60**
			T3-3	Cellophane	58
			T3-4	Rayon	56
			T3-5	Cellophane	56
			T3-6	Cellophane	55
			T3-7	Cellophane	54
			T3-8	Cellophane	49
			T3-9	Cellophane	41
			T3-10	Cellophane	35
			T3-11	Cellophane	35
			T3-12	Cellophane	29
			T3-13	Coal Tar Oil	25
Rio Grande, Albuquerque (R4)	101	10	R4-1	Poly(Styrene), Atactic	50
			R4-2	Poly(Styrene:Vinyldiene Chloride)	41
			R4-3	Rayon	38
			R4-4	Cellophane	38
			R4-5	Endothermic Foaming Agent #2	33
			R4-6	5-Phenyltetrazole, Calcium Salt	31
			R4-7	Poly(Styrene), Atactic	28
			R4-8	N,N-Diphenyl-P-Phenylenediamine	28
			R4-9	Zinc Borate #1	27
			R4-10	Basic Lead Carbonate	20
Rio Grande, Albuquerque (R5)	12	5	R5-1	Rayon	52
			R5-2	Cellophane	44
			R5-3	Poly(Styrene), Atactic	42
			R5-4	Rayon	38
			R5-5	Cellophane	33
Rio Grande, Albuquerque (R6)	96	10	**R6-1**	**Polyamide 6+Polyamide 6,6**	**73**
			R6-2	**Cellophane**	**72**
			R6-3	Polytetrafluoroethylene #4	58
			R6-4	Cellophane	53
			R6-5	Zinc Molybdate on Talc	46
			R6-6	Rayon	41
			R6-7	Polystyrene #1	38
			R6-8	Poly(Styrene:Vinyldiene Chloride)	37
			R6-9	Poly(Styrene:4-Vinylpyridine)	36
			R6-10	Benzyl Alcohol	32
Laboratory Control	18	5	Lab Ctrl-1	Titanium Oxide (98%), Aluminum Oxide (2%)	55
			Lab Ctrl-2	Titanium Oxide (98%), Aluminum Oxide (2%)	50
			Lab Ctrl-3	Titanium Oxide (98%), Aluminum Oxide (2%)	47
			Lab Ctrl-4	Titanium Oxide (98%), Aluminum Oxide (2%)	46
			Lab Ctrl-5	Titanium Oxide (98%), Aluminum Oxide (2%)	41.35
Field Control	15	5	Ctrl-1	Cellophane	50
			Ctrl-2	Poly(Styrene:4-Vinylpyridine)	34
			Ctrl-3	Poly(Styrene:Vinylidene Chloride)	32
			Ctrl-4	2,2-Ethylidene-Bis(4,6-Di-t-Butyl-Phenyl) Fluorophosphonite	25
			Ctrl-5	Bis [2-Hydroxy-5-T-Octyl-3-(Benzotriazol-2-Phenyl] Methane	25

The criteria used in this study require spectra matches >60% for a particle to be considered a confirmed MP. Particles in bold font are particles with a match >60%.

In Laguna Pueblo, NM, a range from 7 to 149 particles/L was detected in the water samples taken from six different locations (Supplementary Fig. S1A–F and Supplementary Table S1 in the Supplementary Data). Water samples taken from three different locations of Tingley Beach, Albuquerque, NM, showed a range of 18–127 particles/L. Finally, a range from 12 to 101 particles/L was detected in water samples taken from three different locations of Rio Grande, Albuquerque, NM.

Following quantification, ATR-FTIR analyses were performed to analyze the chemical composition of the particles. A total of 25, 23, and 25 particles were analyzed from the Laguna Pueblo, Tingley Beach, and Rio Grande samples, respectively. Figure 1 shows representative particles analyzed with ATR-FTIR, Table 1 shows the spectra match of each particle analyzed, and all data from these analyses are available in the Supplementary Data (Supplementary Tables S4–S6 in the Supplementary Data). The criteria used in this study require spectra matches >60% for a particle to be considered a confirmed MP. The 25 particles analyzed from the Laguna Pueblo samples indicated spectra matching from 21% to 72%, relative to pure polymers. Two confirmed MPs were identified at the site- one rayon (72%) and one cellophane (67%) of the 25 particles examined.

Analysis of 23 particles randomly selected from the Tingley Beach samples indicated their spectra matched pure polymers from 25% to 73% (Table 1). Five confirmed MPs were found in these samples, including two polyester (both 73%), two rayon (67% and 63%), and one polytetrafluoroethylene (PTFE) #4 (65%), meaning that 32% of the examined particles match with a polymer spectrum. Finally, the analyses of 25 particles selected from the Rio Grande samples indicated their spectra matched from 20% to 73%, relative to pure polymers. One polyamide (PA) 6+PA 6,6 (73%) particle and one cellophane (72%) particle were confirmed as MPs from the 25 examined particles, indicating 8% of analyzed particles matched with a polymer spectrum. This analysis indicates that Tingley beach, a stagnant freshwater body located in an urban center, contained the highest number of particles confirmed as MPs.

However, a distinction must be made that the ATR-FTIR analysis provides insight specifically into MPs >20 μm.

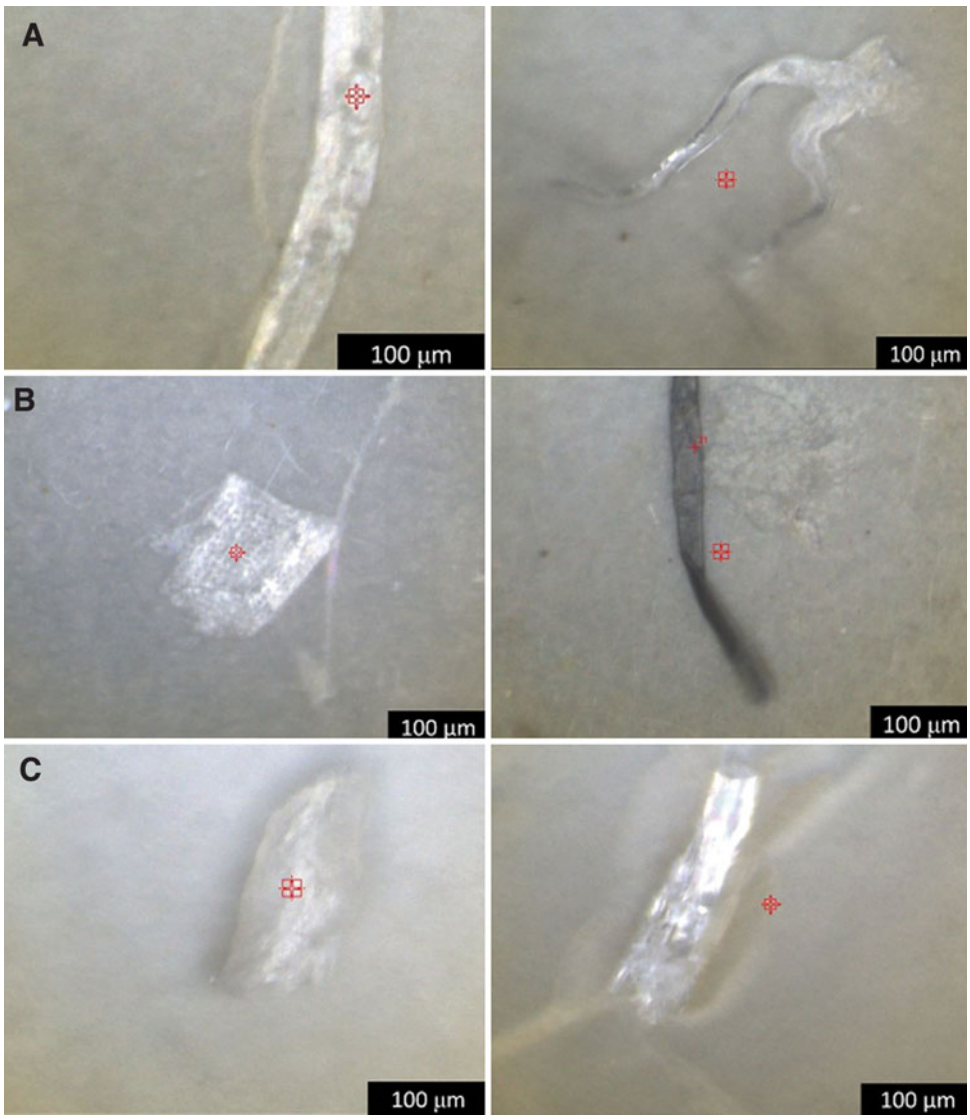

FIG. 1. Representative images of plastic-like particles found in **(A)** Laguna Pueblo, New Mexico (Site L5), **(B)** Tingley Beach, Albuquerque, New Mexico (Site T1 and T2), and **(C)** the Rio Grande, Albuquerque, New Mexico (Site R1 and R3).

While this is limiting, it is important to recall that larger MPs can continue to break down in the environment, potentially releasing micro- and nanoplastics below this 20 μm threshold; thus, an analysis of larger MPs still provides valuable insight. Many of the particles on each filter, especially fibers, had at least one dimension below the 20 μm detection limit of the μ-FTIR, but above the 0.5 μm detection limit of the fluorescence microscope—meaning they could be quantified, but were not eligible for ATR-FTIR analysis. An example of fibrous particles, potentially MPs, which were below the detection limit, is shown in Supplementary Fig. S1 in the Supplementary Data.

Previous studies have also found similar polymer types, including polyester (PES), PA, rayon, or cellophane (CP), and a similar particle content in freshwater. For example, a range from 3.4 to 25.8 particles/L was found in Lake Taihu in China. The most common polymer types identified were CP, PET, PES, PP, and PA (Su et al., 2016).

Fibrous and fragmented MPs were found along the middle and lower reaches of the Yangtze River Basin with concentrations varying from 0.24 to 1.8 particles/L and 0.5 to 3.1 particles/L, respectively (Li et al., 2019; Su et al., 2018). Mainly PP, PE, and polycarbonate (PC) were found in the middle of the Yangtze River Basin (Li et al., 2019), while the most dominant polymers were PES (33%), PP (19%), and PE (9%) in the lower basin area (Su et al., 2018). Similarly, a range from 0.9 to 2.4 particles/L was identified in Suzhou River, Huangpu River, and the urban creeks of Shanghai where the dominant polymer was PES (Luo et al., 2019).

MP functional chemistry. The degradation of MPs in the environment due to ultraviolet (UV) and physical weathering has become well documented in recent years (Liu et al., 2020). In this work, the functional chemistry of weathered environmental MPs is compared with pristine and pure polymer spectral reference libraries. The ATR-FTIR spectra of selected MPs found in field samples compared to the reference spectra are shown in Fig. 2. All examined spectra, including library references, are found in from Supplementary Tables S4 to S6 in the Supplementary Data. Changes in the spectra of MPs found in the samples compared to the reference spectrum may be explained due to weathering patterns, and reactions with other elements in the environment can be observed in the rayon particles (T1-1 and T2-3) in O-H region (3,700–3,000 cm^{-1}) and C-H peaks (2,900 cm^{-1}).

Cellophane particles (T1–2 and T1-3) showed changes in the C-H bending signal (1,450–1,500 cm^{-1}). Other examples include the polyester MPs (T2-1 and T22) with modifications in the O-H (3,700–3,000 cm^{-1}) and C-H peaks (2,900 cm^{-1}) compared to the reference. Discrepancy in functional chemistry between the pristine reference spectra and weathered environmental MPs likely leads to the misidentification or underidentification of MPs by current spectral identification tools. The current challenges of spectral identification highlight the need to generate more environmentally relevant spectral libraries that contain mechanically weathered and UV aged polymers.

Quantification of U and As in freshwater. Our analyses confirmed occurrence of U and As in all freshwaters that were sampled to detect MPs (Supplementary Table S3 in the Supplementary Data). In Laguna Pueblo, the concentration of U ranged from 0.002 to 1.398 μM (0.45–332.80 μg/L) and As from 0.009 to 0.064 μM (0.66–5.54 μg/L). These analyses agree with previous findings (Blake et al., 2017; Blake et al., 2015). The concentration of U and As of samples collected from Tingley Beach ranged from 0.009 to 0.010 μM (2.16 to 2.35 μg/L) of U and 0.143 to 0.152 μM (10.75 to 11.40 μg/L) of As. Samples collected from Rio Grande showed a concentration of U from 0.004 to 0.006 μM (1.07 to 1.43 μg/L), while the concentration of As ranged from 0.031 to 0.041 μM (2.32 to 3.05 μg/L).

In our study, it was not possible to detect accumulation of U and As on the surface of MPs due to the methodologies used for extraction of MPs, that is, in bodies of water with higher content of organic matter and suspended solids, chemical treatment is necessary to remove excess of particulate material. The high content of organic matter and inorganic particles in the samples interfered with the direct analysis of MPs without any sample treatment. However, other studies that have sampled larger plastic pieces, and therefore avoided using chemical separation processes, have demonstrated the association of heavy metals and MPs from samples collected from the environment (Brennecke et al., 2016; Catrouillet et al., 2021; Munier and Bendell, 2018; Rochman et al.,

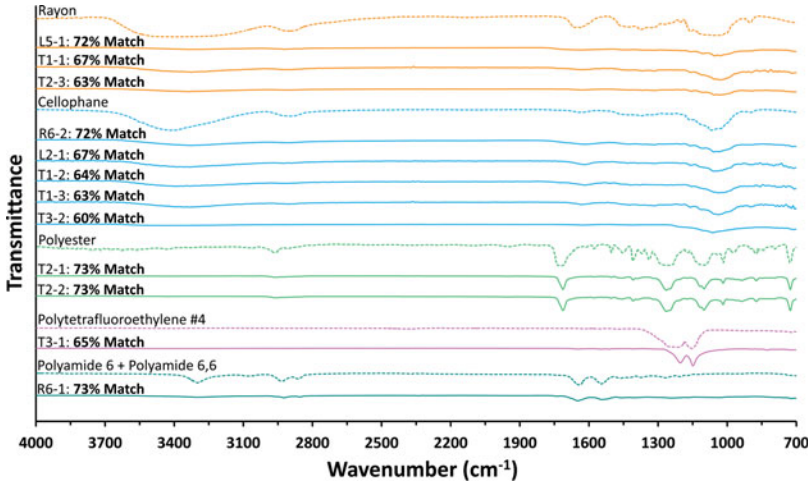

FIG. 2. Infrared spectra of confirmed MPs. *Dotted lines* indicate polymer reference spectra. Images of MP particles L5-1, T1-1, T2-3, R6-2, L2-1, T1-2, T1-3, T3-2, T2-1, T2-2, T3-1, and R6-1 are available in the Supplementary Data. MPs, microplastics.

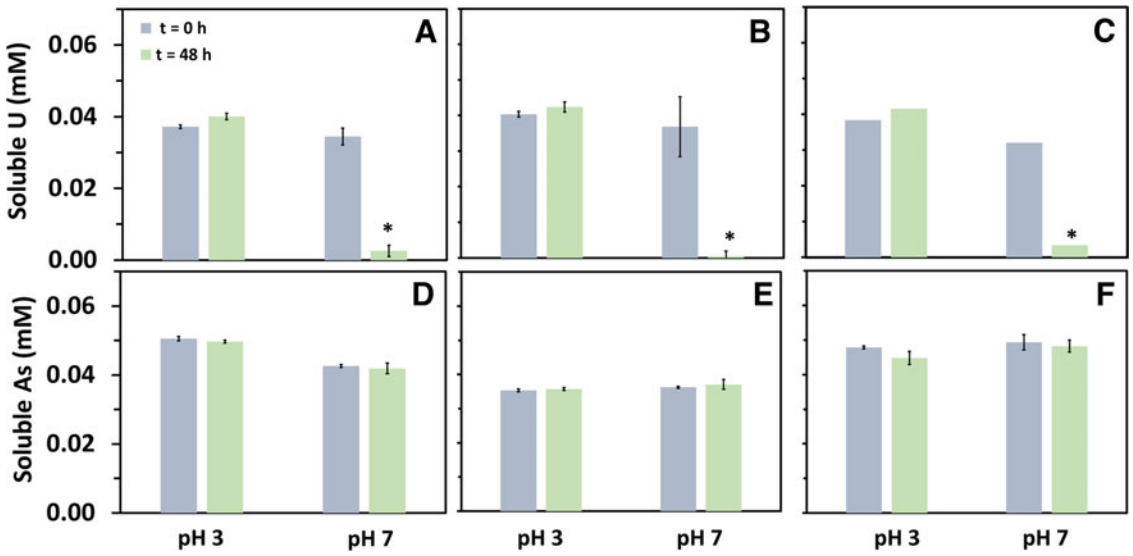

FIG. 3. Soluble U concentration in batch experiments containing **(A)** PMMA, **(B)** PE, and **(C)** PS and soluble As concentration in batch experiments containing **(D)** PMMA, **(E)** PE, and **(F)** control without MPs at pH 3 and pH 7 at 0 and a 48-h exposure. Assays were supplied with 0.05 mM U. Error bars indicate standard deviation obtained from duplicates. *Asterisks* represent the significant difference of soluble U concentration. PE, polyethylene; PMMA, polymethyl(meta)acrylate; PS, polystyrene.

2014). These field observations motivated additional experiments in controlled laboratory conditions to assess interactions of metals with MPs.

Interfacial interactions of metals and MP in controlled laboratory conditions

Uranium precipitation and reactivity with the MP surface at pH 7. The reactivity of U and MPs depended on the pH. In assays supplied with PMMA and PE carried out at pH 7, the soluble concentration of U decreased significantly ($p < 0.05$) from 0.05 to $\sim$0.003 mM after 48 h of reaction (Fig. 3A–C). Surface SEM EDS analyses revealed that U precipitated on the surface of PMMA (Fig. 4A). Further TEM analyses of both the surface of the MPs and precipitates formed in the control suggest that the solid phase formed resemble Na-compreignacite on the surface of PMMA (Fig. 4B). Chemical equilibrium analyses were conducted and indicated that the solution was supersaturated with respect to schoepite and Na-compreignacite, both uranyl oxide hydrates.

The Na-bearing U solids were the primary phases in our study because NaOH was used to adjust the pH. The decrease in U observed in the control without MPs at pH 7 was likely caused by homogenous precipitation of uranyl solids. Heterogenous precipitation took place with the presence of MPs, which provided surface sites for U solids to deposit and precipitate. These results suggest that U homogenous and heterogenous precipitation processes are relevant mechanisms that may be observed in aquatic environments supersaturated with U. Past studies have confirmed Na-compreignacite and schoepite precipitates formed at pH 7 in a similar concentration used in our study (Gorman-Lewis, Burns, et al., 2008; Gorman-Lewis, Fein, et al., 2008; Kanematsu et al., 2014).

To further investigate the surface interaction mechanism of U and MPs, PMMA MPs were exposed to three different U concentrations (0.05, 0.1, and 0.2 mM) at pH 7 for 48 h. PMMA MPs were selected for these experiments because they have the smallest particle size (1–45 μm), largest surface area (0.86 ± 0.87 m^2/g), most negatively charged surface (-42.83 ± 5.17 mV) compared to PE and PS at pH 7 (Supplementary Table S2 and Supplementary Fig. S2 in the Supplementary Data), and the concentration of U decreased the most in the sorption experiments amended with PMMA MPs. The soluble U concentration significantly ($p < 0.05$) decreased in assays supplied with and control without PMMA MPs (Fig. 5). These findings show that homogenous and heterogenous precipitation of U onto the surface of MPs are key mechanism for U reactivity in the system studied.

Interaction of MPs with prefiltered U solutions. Additional experiments were run with U concentrations of 0.02 and 0.06 mM, which were prefiltered to ensure that U precipitates were the conduct in which U interacted with MP and not the soluble fraction. The filtered U solution exposed to the three MPs and the control at pH 7 slightly decreased (Supplementary Fig. S4 in the Supplementary Data). The use of glass vials was eliminated in this section as it can influence precipitation reactions; PP tubes was used instead. These findings imply that homogenous and heterogenous precipitation are still occurring in the system even with the substitution from glass to plastic and with the extra filtration step to remove U precipitate before MP exposure.

Although U precipitated homogenously in the control without MPs, the SEM analyses confirmed U mineral precipitated heterogeneously on the MP surface. The EDS analyses also showed U and Na compositions and did not show any silica (Si) (Fig. 4). A paired-samples *t*-test showed the decrease of U concentration is significantly different, $t(2) = 64.27$, $p = 0.0002$, ($p < 0.05$). Our results demonstrate that the precipitation process drives the interaction between the MPs and uranium, and not the soluble ions in the system.

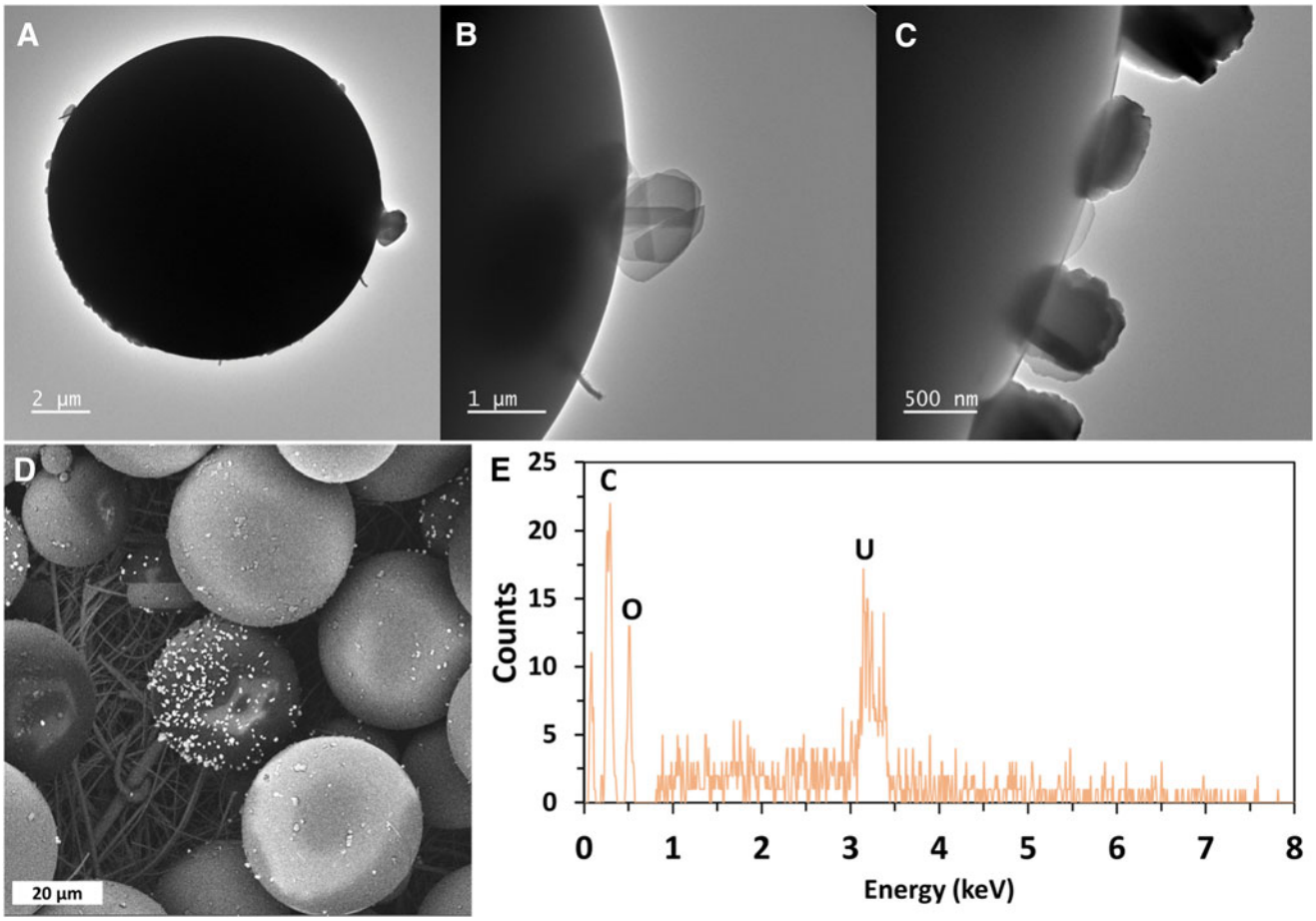

FIG. 4. Spectroscopy analyses of PMMA MPs exposed to 0.06 mM of U for 48 h experiments were performed at pH 7, (**A–C**) TEM images of precipitates onto the commercial PMMA MP surface and (**D, E**) SEM/EDS analyses confirming U accumulated on the MP surface. EDS, Energy Dispersive Spectroscopy; SEM, Scanning Electron Microscopy; TEM, Transmission Electron Microscopy.

Other studies have reported that metals interacted with MPs. Most interactions reported in these studies are attributed to adsorption reactions between cations and MPs (Godoy et al., 2019; Munier and Bendell, 2018; Rochman et al., 2014; Zou et al., 2020).

Lack of reactivity of As (pH 3 and 7) and U (pH 3) with MPs. All experiments supplied with As and PE, PS, and PMMA MPs at pH 3 and pH 7 remained close to the initial concentration (0.05 mM) after the 48 h of exposure (Fig. 3D–F). Similar results were found for the assays supplied with U

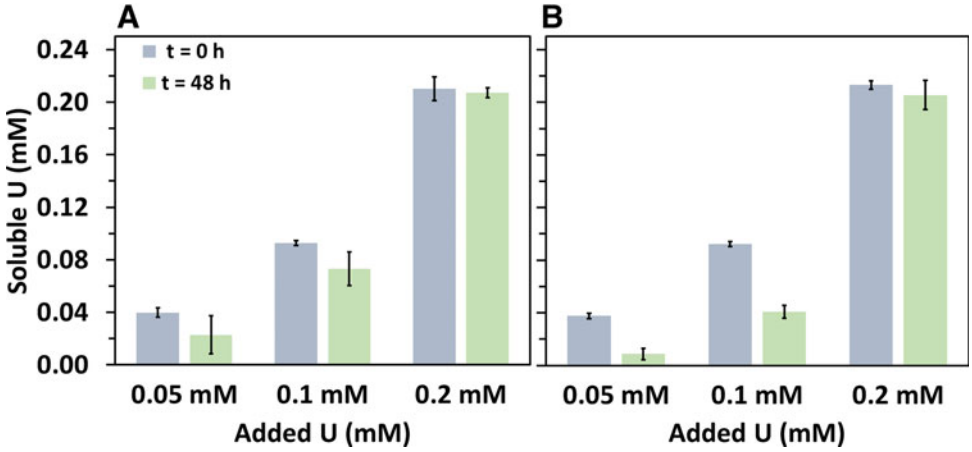

FIG. 5. Soluble U concentration in batch experiments containing **(A)** PMMA and **(B)** control (no MPs) at pH 7 at 0 and a 48-h exposure. Error bars indicate standard deviation obtained from triplicates.

at pH 3. The controls showed no change in the concentration as well.

Although sorption of As (III) onto PTFE and PS MPs at pH ranging from 3 to 7 has been reported (Dong et al., 2020; Dong et al., 2019), we found no sorption of As (V) onto MPs at pH 3 and 7. Lack of sorption of As (V) may be explained by difference of charges; that is, As (V) is predominantly negative at this pH range ($H_2AsO_4^-$ and $HAsO_4^{2-}$), whereas As (III) species are uncharged (Benjamin, 2014). Lack of sorption of U at pH 3, predominantly UO_2^{2+} at acidic pH, likely results from the lack of electrostatic attraction as well. Previous studies have stated that hydrophobic and electrostatic interactions are two predominant mechanisms for the sorption of contaminants on MPs (Tourinho et al., 2019).

Environmental implications

Freshwater samples containing MPs and taken from a location that has been historically affected by U mining highlight the importance of detecting MPs on sites also affected by other contaminants of concern. Accumulation of contaminants on MPs can facilitate the transport and localized consumption of contaminants by various trophic groups. Moreover, the batch experiment data indicated that heterogeneous precipitation could be a key reaction mechanism between MPs and U, which is relevant in sites with elevated concentrations of metals (Blake et al., 2017; Donahue and Hendry, 2003; Ruiz et al., 2016).

Our results do not infer that MPs induce precipitation of U; precipitation of U occurs in supersaturated conditions (Meza et al., 2023); however, if MPs occur in sites where high concentrations of U are also present, precipitation onto the surface of MPs is a potential mechanism by which MPs interact with metals. These findings are relevant and unique because all previous studies have focused on adsorption reactions, while in our study, we showed that precipitation is also a plausible interaction mechanism between metals and MP. Enhanced precipitation or sorption of U and As onto MPs may be likely observed in weathered MP compared to pristine polymers, which are generally less oxidized and thus less reactive than those of environmental MPs (Liu et al., 2020; Yousif and Haddad, 2013). In El Hayek et al. (2023), we observed that UV aging modifies the functional chemistry of PS beads.

Actual environmental conditions (e.g., pH, organic matter composition, ionic strength, salinity, contact time, and temperature) may affect these reactions; therefore, future research should observe the behavior of MPs and U with weathered MPs and in various aqueous media like samples collected from freshwater and seawater. Actual environmental conditions (e.g., pH, organic matter composition, ionic strength, salinity, contact time, and temperature) may affect these reactions; therefore, future research should observe the behavior of MPs and U with weathered MPs and in various aqueous media like samples collected from freshwater and seawater. A better understanding of the relationship and behavior of metals and MPs would provide valuable information about the transport of contaminants sorbed onto MPs and potential toxicity synergies.

Conclusions

Our findings indicate that heavy metal contaminated in freshwater rural communities can be also affected by MP occurrence. Although urban sites contained more confirmed MPs, freshwater in the rural community also contained MPs. Fluorescence quantification of MPs indicated that all water samples contained MPs in the range of 7 to149 particles/L. Further ATR-FTIR analyses of some of the detected particles confirmed their chemical compositions match with known polymer spectra and displayed clear discrepancies in surface chemistry, likely due to environmental exposure. Tingley beach, a stagnant water reservoir located in an urban center, contained the highest amount of confirmed MP particles.

Laboratory experiments evidenced the deposition of U precipitates onto the surface of MPs at pH 7, indicating that MPs can also interact with metals through other mechanisms aside adsorption. Chemical speciation modeling and TEM analyses suggest that the U solids formed are sodium-compreignacite and schoepite. The lack of interfacial interaction of As and U with commercial MPs (i.e., PMMA, PE, and PS) at pH 3 is explained by unstable surface charge of the MPs. Lack of interaction of As and MPs at pH 7 is likely explained by the charge repulsion of As (anionic metalloids) and the negative surface of MPs. Our study provides insights about occurrence of MPs, the interfacial interaction of U and As with MPs in laboratory-controlled conditions, and information about their fate, mobility, and potential synergies in the environment.

Acknowledgments

The content, opinions, findings, conclusions, and recommendations are those of the authors and do not necessarily represent the official views of any of the institutions mentioned.

Authors' Contributions

J.Q.: investigation, formal analysis, and writing—original draft; K.H.: investigation, formal analysis, and writing—review and editing; S.J.: investigation; E.E.H.: investigation; A.N.: investigation and resources; A.-M.S.A.: resources; M.S.: resources; A.B.: resources; P.L/: formal analysis; J.M.C.: conceptualization, methodology, writing—review and editing, supervision, resources, and funding acquisition; K.J.H.: conceptualization, methodology, writing—review and editing, supervision, resources, and funding acquisition; J.G.-E.: conceptualization, methodology, writing—review and editing, supervision, resources, project administration, and funding acquisition.

Author Disclosure Statement

No competing financial interests exist.

Funding Information

This work was funded by the Center for Water and the Environment (National Science Foundation CREST Grant No. 1914490), National Institute of Environmental Health Sciences (NIEHS) Superfund Research Program (Award 1 P42 ES025589), the National Institute on Minority Health and Health Disparities (NIMHD) Award Number P50MD015706, and the New Mexico Water Resources Research Institute, the NM State Legislature (NMWRRI-SG-2020). The acquisition of the JEOL NEOARM AC-STEM at the University of New Mexico was supported by NSF DMR-1828731.

Supplementary Material

Supplementary Data

References

Andrady AL, Neal MA. Applications and societal benefits of plastics. Philos Trans R Soc B: Biol Sci 2009;364(1526): 1977–1984.

Ateia M, Ersan G, Gar Alalm M, et al. Emerging investigator series: Microplastics sources, fate, toxicity, detection, and interactions with micropollutants in aquatic ecosystems—A review of reviews. Environ Sci Proc Imp 2022;24:172–195; doi: 10.1039/d1em00443c

Benjamin MM. Water chemistry. Waveland Press, Inc: Long Grove Illinois, USA; 2014.

Blake JM, Avasarala S, Artyushkova K, et al. Elevated concentrations of U and co-occurring metals in abandoned mine wastes in a northeastern Arizona Native American community. Environ Sci Technol 2015;49(14):8506–8514; doi: 10 .1021/acs.est.5b01408

Blake JM, De Vore CL, Avasarala S, et al. Uranium mobility and accumulation along the Rio Paguate, Jackpile Mine in Laguna Pueblo, NM. Environ Sci Proc Imp 2017;19(4):605–621; doi: 10.1039/C6EM00612D

Blettler MCM, Abrial E, Khan FR, et al. Freshwater plastic pollution: Recognizing research biases and identifying knowledge gaps. Water Res 2018;143:416–424; doi: 10.1016/j.watres.2018.06.015

Brennecke D, Duarte B, Paiva F, et al. Microplastics as vector for heavy metal contamination from the marine environment. Estuar Coast Shelf S 2016;178:189–195; doi: 10.1016/j.ecss .2015.12.003

Carbery M, O'Connor W, Palanisami T. Trophic transfer of microplastics and mixed contaminants in the marine food web and implications for human health. Environ Intl 2018;115: 400–409; doi: 10.1016/j.envint.2018.03.007

Catrouillet C, Davranche M, Khatib I, et al. Metals in microplastics: Determining which are additive, adsorbed, and bioavailable. Environ Sci Proc Imp 2021;23(4):553–558; doi: 10.1039/D1EM00017A

Di M, Wang J. Microplastics in surface waters and sediments of the Three Gorges Reservoir, China. Sci Total Environ 2018;616–617:1620–1627; doi: 10.1016/j.scitotenv.2017 .10.150

Donahue R, Hendry MJ. Geochemistry of arsenic in uranium mine mill tailings, Saskatchewan, Canada. Appl Geochem 2003;18(11):1733–1750; doi: 10.1016/S0883-2927(03)00106-9

Dong Y, Gao M, Song Z, et al. Adsorption mechanism of As(III) on polytetrafluoroethylene particles of different size. Environ Pollut 2019;254:112950.

Dong Y, Gao M, Song Z, et al. As(III) adsorption onto different-sized polystyrene microplastic particles and its mechanism. Chemosphere 2020;239:124792.

Eerkes-Medrano D, Thompson RC, Aldridge DC. Microplastics in freshwater systems: A review of the emerging threats, identification of knowledge gaps and prioritisation of research needs. Water Res 2015;75:63–82.

El Hayek E, Castillo E, In JG, et al. Photoaging of polystyrene microspheres causes oxidative alterations to surface physicochemistry and enhances airway epithelial toxicity. Toxicol Sci 2023;193(1):90–102; doi: 10.1093/toxsci/kfad023

Godoy V, Blázquez G, Calero M, et al. The potential of microplastics as carriers of metals. Environ Pollut 2019;255(Pt 3): 113363; doi: 10.1016/j.envpol.2019.113363

Gonzalez-Estrella J, Meza I, Burns AJ, et al. Effect of bicarbonate, calcium, and pH on the reactivity of As(V) and U(VI) mixtures. Environ Sci Technol 2020;54(7):3979–3987; doi: 10.1021/acs.est.9b06063

Gorman-Lewis D, Burns PC, Fein JB. Review of uranyl mineral solubility measurements. J Chem Thermodyn 2008;40(3): 335–352.

Gorman-Lewis D, Fein JB, Burns PC, et al. Solubility measurements of the uranyl oxide hydrate phases metaschoepite, compreignacite, Na–compreignacite, becquerelite, and clarkeite. J Chem Thermodyn 2008;40(6):980–990.

Holmes LA, Turner A, Thompson RC. Interactions between trace metals and plastic production pellets under estuarine conditions. Mar Chem 2014;167:25–32; doi: 10.1016/j .marchem.2014.06.001

Kanematsu M, Perdrial N, Um W, et al. Influence of phosphate and silica on U(VI) precipitation from acidic and neutralized wastewaters. Environ Sci Technol 2014;48(11):6097–6106.

Koelmans AA, Mohamed Nor NH, Hermsen E, et al. Microplastics in freshwaters and drinking water: Critical review and assessment of data quality. Water Res 2019;155:410–422; doi: 10.1016/j.watres.2019.02.054

Lenaker PL, Baldwin AK, Corsi SR, et al. Vertical distribution of microplastics in the water column and surficial sediment from the Milwaukee River Basin to Lake Michigan. Environ Sci Technol 2019;53(21):12227–12237; doi: 10.1021/acs.est .9b03850

Li C, Busquets R, Campos LC. Assessment of microplastics in freshwater systems: A review. Sci Total Environ 2020;707:135578; doi: 10.1016/j.scitotenv.2019.135578

Li J, Liu H, Paul Chen J. Microplastics in freshwater systems: A review on occurrence, environmental effects, and methods for microplastics detection. Water Res 2018;137:362–374; doi: 10.1016/j.watres.2017.12.056

Li L, Geng S, Wu C, et al. Microplastics contamination in different trophic state lakes along the middle and lower reaches of Yangtze River Basin. Environ Pollut 2019;254:112951; doi: 10.1016/j.envpol.2019.07.119

Liu P, Zhan X, Wu X, et al. Effect of weathering on environmental behavior of microplastics: Properties, sorption and potential risks. Chemosphere 2020;242:125193; doi: 10.1016/j.chemosphere.2019.125193

Luo W, Su L, Craig NJ, et al. Comparison of microplastic pollution in different water bodies from urban creeks to coastal waters. Environ Pollut 2019;246:174–182; doi: 10 .1016/J.ENVPOL.2018.11.081

Meza I, Gonzalez-Estrella J, Burns PC, et al. Solubility and thermodynamic investigation of meta-autunite group uranyl arsenate solids with monovalent cations Na and K. Environ Sci Technol 2023;57(1):255–265; doi: 10.1021/acs.est .2c06648

Munier B, Bendell LI. Macro and micro plastics sorb and desorb metals and act as a point source of trace metals to coastal ecosystems. PLoS One 2018;13(2):e0191759; doi: 10.1371/journal.pone.0191759

Nafiaah N. Interaction of freshwater microplastics with biota and heavy metals: A review. Environ Chem Lett 2020;18(6):1813–1824; doi: 10.1007/s10311-020-01044-3

Prata JC, Alves JR, da Costa JP, et al. Major factors influencing the quantification of Nile Red stained microplastics and improved automatic quantification (MP-VAT 2.0). Sci Total Environ 2020;719:137498; doi: 10.1016/j.scitotenv.2020.137498

Robertson J, Hendry MJ, Kotzer T, et al. Geochemistry of uranium mill tailings in the Athabasca Basin, Saskatchewan,

Canada: A review. Crit Rev Env Sci Tec 2019;49(14):1–57; doi: 10.1080/10643389.2019.1571352

Rochman CM, Hentschel BT, Teh SJ. Long-term sorption of metals is similar among plastic types: Implications for plastic debris in aquatic environments. PLoS One 2014;9(1):e85433; doi: 10.1371/journal.pone.0085433

Ruiz O, Thomson BM, Cerrato JM. Investigation of in situ leach (ISL) mining of uranium in New Mexico and post-mining reclamation. N M Geol 2016;38(4):77–85.

Su L, Cai H, Kolandhasamy P, et al. Using the Asian clam as an indicator of microplastic pollution in freshwater ecosystems. Environ Pollut 2018;234:347–355; doi: 10.1016/J.ENVPOL.2017.11.075

Su L, Xue Y, Li L, et al. Microplastics in Taihu Lake, China. Environ Pollut 2016;216:711–719; doi: 10.1016/J.ENVPOL.2016.06.036

Tourinho PS, Kočí V, Loureiro S, et al. Partitioning of chemical contaminants to microplastics: Sorption mechanisms, environmental distribution and effects on toxicity and bioaccumulation. Environ Pollut 2019;252:1246–1256; doi: 10.1016/j.envpol.2019.06.030

Wong JKH, Lee KK, Tang KHD, et al. Microplastics in the freshwater and terrestrial environments: Prevalence, fates, impacts and sustainable solutions. Sci Total Environ 2020;719:137512; doi: 10.1016/j.scitotenv.2020.137512

Yang L, Luo W, Zhao P, et al. Microplastics in the Koshi River, a remote alpine river crossing the Himalayas from China to Nepal. Environ Pollut 2021;290:118121; doi: 10.1016/j.envpol.2021.118121

Yonkos LT, Friedel EA, Perez-Reyes AC, et al. Microplastics in four estuarine rivers in the Chesapeake Bay, U.S.A. Environ Sci Technol 2014;48(24):14195–14202; doi: 10.1021/es5036317

Yousif E, Haddad R. Photodegradation and photostabilization of polymers, especially polystyrene: Review. SpringerPlus 2013;2(1):398; doi: 10.1186/2193-1801-2-398

Zou J, Liu X, Zhang D, et al. Adsorption of three bivalent metals by four chemical distinct microplastics. Chemosphere 2020;248:126064; doi: 10.1016/j.chemosphere.2020.126064